J Nanostruct 12(4): 1034-1048, Autumn 2022

RESEARCH PAPER

Broccoli–like Iron Oxide Nanoparticles Synthesis in Presence of Surfactants and Using Them in the Removal of Water-Colored Contamination

Hussein M. Mohammad , Shaymaa I. Saeed, Luma M. Ahmed *

Department of Chemistry, College of Science, University of Kerbala, 56001, Iraq

ARTICLE INFO

Article History:
Received 24 June 2022
Accepted 26 September 2022
Published 01 October 2022

Keywords:
CTAB
Eosin Yellow Dye
Magnetite
Nanoparticles
SDS
Triton X 100

ABSTRACT

Magnetic iron oxide nanoparticles (Fe_3O_4 NPs) were synthesized by novel precipitation method as inverse spinel (Fe_2O_3. FeO). They are directly prepared without calcination under oxygen gas. The Fe_3O_4 NPs had been prepared by combining the iron sulfate solution with the aqueous mixture including sodium hydroxide and sodium nitrate, without and with using various surfactants such as sodium dodecyl sulfate (SDS), triton X100, cetrimonium bromide (CTAB) and cetramide (CT) as templates. The FT-IR analysis demonstrated the Fe-O octahedral and tetrahedral bending at 744 cm^{-1} and 598 cm^{-1} respectively. The XRD analysis discovered the mean crystal size of Fe_3O_4 NPs is smaller than that presence of surfactants, and its value increment from 8.5 nm for Fe_3O_4 NPs to 21.55 nm, 22.53 nm, 27.66 nm, and 27.72 nm for Fe_3O_4 + Triton X-100, Fe_3O_4 + CT, Fe_3O_4 + SDS, and Fe_3O_4 + CTAB, respectively. SEM revealed their samples are nanoparticles and aggregated together like broccoli. The possibility of using Fe_3O_4 NPs as magnetic adsorbents to remove the eosin yellow dye from aqueous solutions was successes and economy, due to collect by magnets without need for a long time to separate with centrifuge or filter paper. The maximum chemisorption of dye was 94.48 % using Fe_3O_4 NPs + CT at shaking 1hour, because CT has a positive part as a hydrophilic moiety and the used dye is acidic nature so will attract and dye easy removal, and the reuse reached to five times with efficiency depressed to 75.61 %.

How to cite this article
Mohammad H M., Saeed S I., Ahmed L M.. Broccoli–like Iron Oxide Nanoparticles Synthesis in Presence of Surfactants and Using Them in the Removal of Water-Colored Contamination. J Nanostruct, 2022; 12(4):1034-1048. DOI: 10.22052/JNS.2022.04.024

INTRODUCTION

Iron oxides are among the most important transition metal oxides in terms of technological significance. To date, sixteen pure phases of iron oxides, i.e. Oxides, hydroxides, or oxy-hydroxides, have been discovered. These are $Fe(OH)_3$, $Fe(OH)_2$, $Fe_5(OH)_8.4H_2O$, metal-Fe_2O_4, FeO. The trivalent state of these oxide compounds is one of their most distinguishing features like normal metal ferrite (M-Fe_2O_4). Iron, low solubility, and brilliant colors[1]. Except for iron oxide, all of the iron oxides are crystalline. The schwertmannite and the ferrihydrite are poorly-crystalline. These oxides can be created using any known wet chemical process. Iron oxide nanoparticles (IONPS) are made up of magnetite (Fe_3O_4) particles with diameters ranging from 1 to 100 nanometers, and are used in magnets. These

* *Corresponding Author Email: luma.ahmed@uokerbala.edu.iq*

nanoparticles are applied in magnetic data storage, bio sensing, drug delivery, and other applications [2]. Approximately 16 different phases of iron oxide have been reported [3], with the exception of schwertmannite and ferri-hydrite, which be crystalline [4], metallic nanoparticle production and use for super paramagnetic properties are common in therapeutic and diagnostic applications such as magnetic resonance imaging (MRI) [5]. These iron oxides are also used as catalysts, sorbents, pigments, flocculants, coatings, gas sensors, wastewater treatment [6] and lubricants [7], based on their superior magnetic properties, these nano particles can also be used in various advanced processes to form nano reactors, added to polymer films, and other products [8]. Magnetite has an inverse spinel structure with alternating octahedral and tetrahedral-octahedral layers [9]. Magnetite, which contains both ferrous (reduced) and ferric (oxidized) iron species, is also known as iron II, III [10]. Due to higher ferrous crystal field stabilization energy (CFSE), ferrous species are observed to occupy half of the octahedral lattice sites. On the other hand, ferric species, occupy the other octahedral lattice [11]. Additionally, magnetite unit cells adhere to the face centred cubic pattern crystal lattice parameter, a = 0.8396[10]. These applications produce magnetite as super magnetic nanoparticles of iron oxide, and there is a need for the development and modification of low-cost synthesis processes.

This study includes preparation of magnetite NPS using a novel method in aqueous solutions without and with using surfactants such as cetrimide (CT), cetrimonium bromide (CTAB) as positive surfactants, sodium dodecyl sulphate (SDS) as a negative surfactant and triton x100 as a non-ionic surfactant. The characterizations of prepared magnetite NPS were investigated using FTIR, XRD, SEM. Based on the addition of surfactants as templates during magnetite NPS, the facial mechanism of ordering nanoparticles as broccoli shape was suggested. The removal process of water colored-contamination was compared without and with using surfactants via prepared of magnetite NPS and study the thermodynamics functions.

MATERIALS AND METHODS

Materials

All chemicals used in this study such as Ferric sulfate $FeSO_4 .7H_2O$, Sodium nitrate $NaNO_3$, Sodium hydroxide NaOH were provided by BDH. The surfactants such as cetramide (CT), sodium dodecyl sulfate (SDS), cetrimonium bromide (CTAB), triton x100 were supplied from Qualikems, DIDACTIC, Interchimiques SA and Sigma-Aldrich companies respectively. The Eosin yellow dye ($C_{20}H_6Br_4Na_2O_5$) has molar mass 691.9g/mole, dye class (Xanthene dye), color (Pink powder and slightly yellowish cast in aqueous solution), and wavelength (516 nm) [12] was equipped by CDH.

Synthesis of Spinel Fe_3O_4 nano crystals

Into a 400 mL beaker, 2.0 g of $FeSO_4 \bullet 7H_2O$ was dissolved in 150 mL of water. Into a 100 mL beaker, 50 mg of $NaNO_3$ and 0.56 g of NaOH were mixed and dissolved in 60 mL of water. Both solutions were heated to 75 ºC separately, and then mixed together using a stirring rod, not a magnetic stirrer bar, for 10 minutes. The later mixture was transferred from the magnetic stirrer using a tong, and a green suspension was produced, and rapidly turned to black color. The black color suspension was continuously heated to 90 ºC for 10 min, then cooled to 20 ºC and the acidify of the mixture was increased by adding 3 M HCl. This black suspension was filtered using a Buchner funnel. The produced black precipitation was washed twice with 50 mL of water to remove all salts, and then dried in an oven at 100 ºC at 60 min. The black powder was scraped of the filter paper as shown in Fig. 1.

The chemical reactions of spinel Fe_3O_4 formed without and with surfactant were suggested using the following chemical reactions.

$$12\ FeSO_4.7H_2O + 23NaOH + NaNO_3 \rightarrow 4Fe_3O_4 + 12Na_2SO_4 + NH_3\uparrow + 94H_2O$$

$$12\ FeSO_4.7H_2O + 23NaOH + NaNO_3 + surfactant \rightarrow 4Fe_3O_4 + 12Na_2SO_4 + NH_3\uparrow + 94H_2O + surfactant$$

Application the Spinel Fe_3O_4 in removal of Eosin yellow dye

A 0.05 g from several samples of prepared Fe_3O_4 without and with of surfactants was added to 100 mL of eosin yellow dye solution in a beaker and shaking using a shakier for 10-60 minutes at 50 rpm and 22 °C. After adsorption of the dye on the Fe_3O_4 surface, both were uptake by the magnet.

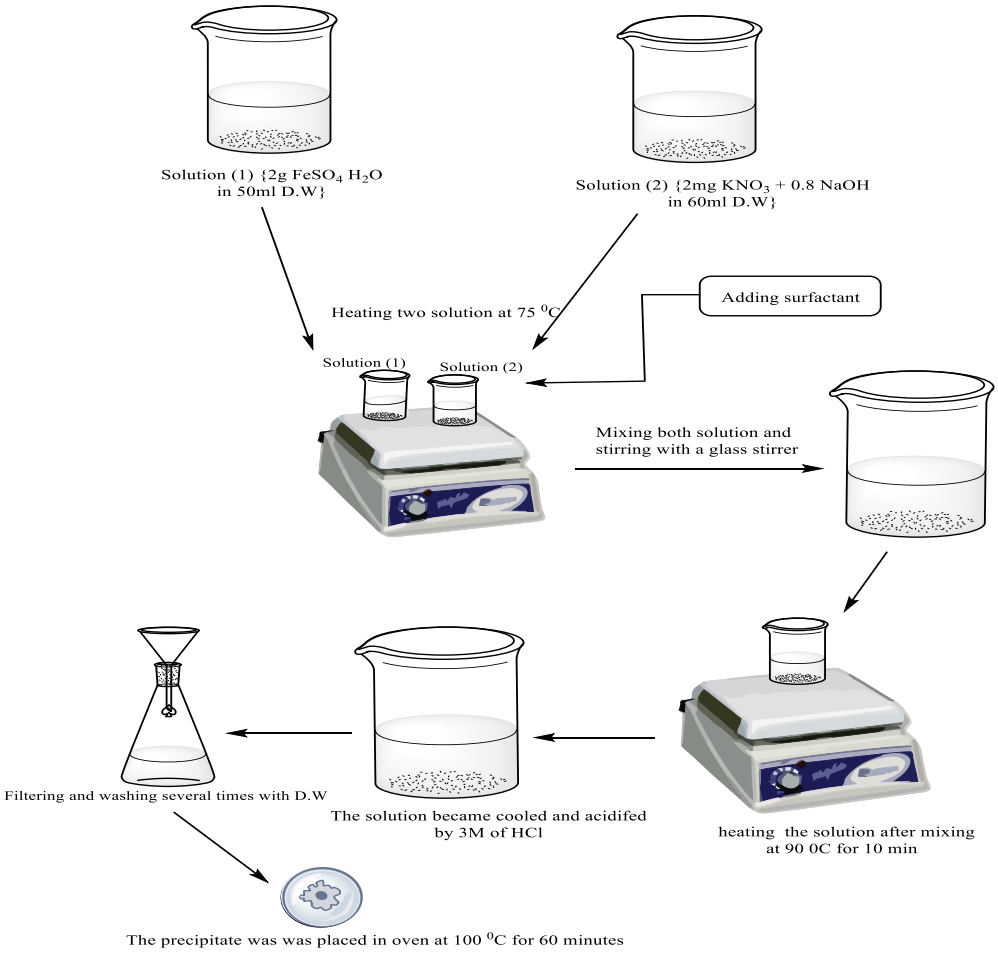

Fig. 1. The schematic diagram of the steps of Fe_3O_4 nanoparticle preparation.

The residue dye concentration after adsorption was measured in solution using UV-visible spectrophotometer at 516 nm, then the amount of adsorption C_r will be calculated. Equations 1 and 2 were used to calculate the dye removal efficiency E% [13-14] and quantity of absorption (q %) [14-15] with different types of synthesized nanoparticles, C_o is the initial concentration of dye.

$$\text{Dye removal efficiency (E \%)} = \frac{(C_o - C_r)}{C_o} \text{ x } 100 \quad (1)$$

$$q\,\% = \frac{(C_o - C_r) * V}{m} \quad (2)$$

RESULTS AND DISCUSSION

Synthesis of Iron oxide NPS

The main objective of this study was to synthesize magnetic iron oxide without and with surfactants (CT, CTAB, SDS, and Triton X-100) through the use of hydrated iron sulfate, where some Fe(II) is converted to Fe(III) by partial oxidation using sodium nitrate and in the presence of the NaOH . The general mechanism of ordering the prepared Fe_3O_4 NPs in presence of surfactants as templates was investigated to give reasonable growth. As displayed in Fig. 2.

Characterization of the prepared Fe_3O_4 nanoparticles

FT-IR Analysis

FTIR spectra are appeared for all magnets prepared in Fig. 3, the broad peak at 3163.36 cm^{-1} assigned to the O - H group, in addition to the peak at 1100 cm^{-1} which is assigned to the O-Fe-O as a octahedron bending. Fe-O bond is located

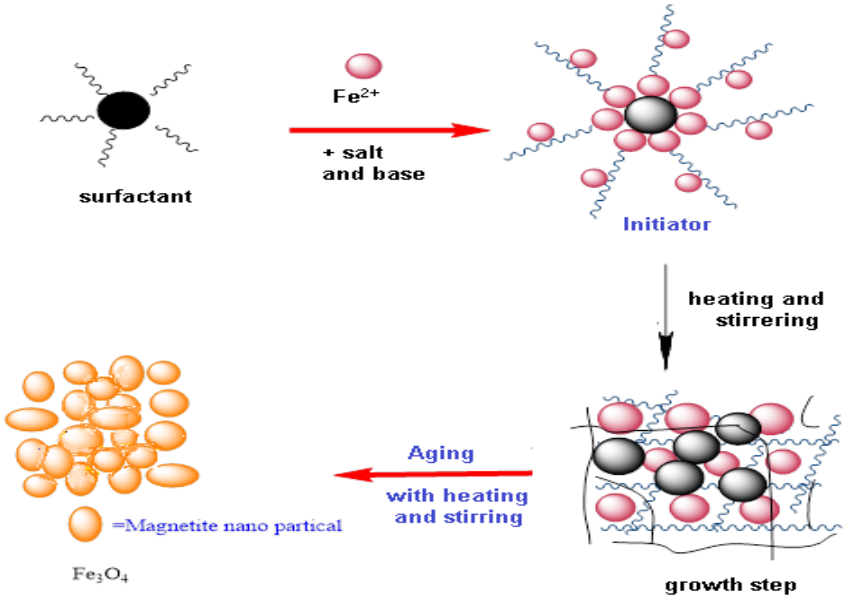

Fig. 2. Magnetic iron oxide nanoparticles in the presence of surfactants (modified from the reference [12]).

between 640 and 598 cm^{-1} which presents to the tetrahedral curvature, Fig. 3, curve B shows the broad peak at 3340 cm^{-1} beyond to the O–H stretching of the iron oxide and another peak at 3028 cm^{-1} is assigned to the N–H bending. In addition to the peaks between 2924 and 2850 cm^{-1} assigned to the stretching of C-H. The peak at 1207 cm^{-1} explains the O–H bending. The more intense bands between 744 and 598 cm^{-1} are represent to the Fe-O octahedral and tetrahedral bending [17].

The same applies to the spectrum of c, d, and e where the same peaks appear in the spectrum of magnetic iron oxide, with the presence of some distinctive peaks which belong to the active groups in the surfactant molecule. The same applies to the spectrum of c, d, and e the same peaks appear in the spectrum of magnetic iron oxide, with the presence of some distinctive peaks that belong to the active groups in the surfactant molecule, such as the peak at 3159 cm^{-1} indicates to the N–H bending, peak at 1111 cm^{-1} demonstrates the O-Fe-O the octahedron bending in fig c and the absorption at 1739 cm^{-1} was caused by C=O stretching in Fig. 3E.

Structure Properties

X-ray diffraction (XRD) measurements were used to obtain the crystal structure of magnetic Fe_3O_4 NP prepared in the without and with of surfactants. Fig. 4 shows that the XRD measurements for all the prepared compounds. In Fig. 4-a, the XRD measurement of the magnetic Fe_3O_4 Np without and with Using any surfactants was observed. The appearance of diffraction peaks at 2θ values of 18.96°(111), 30.4° (220), 35.64° (311), 43.4° (400), 53.16 degrees (422), 57.32 degrees (511), 63.12 degrees (440), and 73.12 degrees (553) are consistent with the standard XRD data of the structure of spinel Fe_3O_4. It was also observed that some peaks disappeared and their relative intensity changed when adding surfactants.

the peak at 2θ values of 18.96 degrees at (111) disappeared when using Triton X100, CT, and CTAB, but the addition of surfactants leads to increase in the relative strength of the peaks at 2 that a 35.64 ° (311), 43.4° (400), 53.16° (422), 57.32° (511), 63.12° (440), and 73.12 ° (553) The prepared nanoparticles in the case of using both CT and CTAB. The Fe_3O_4 nanoparticles for all shapes in Fig. 3 (a) to (e) are well crystalline and the position and the relative intensity of the diffraction peaks match well with the standard phase magnetite NPs diffraction pattern of the International Centre of Diffraction Data card

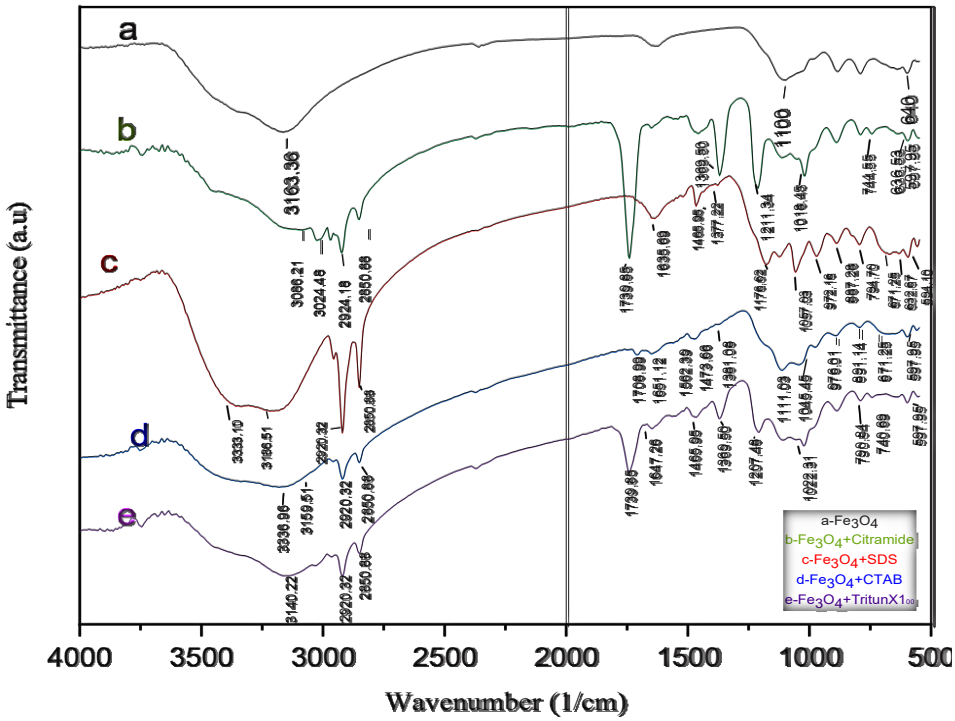

Fig. 3. The FT-IR spectra of prepared Fe_3O_4 without and with surfactants(a) Fe_3O_4 without surfactant, (b) Fe_3O_4+CT, (c) Fe_3O_4+ CTAB , (d) Fe_3O_4+SDS, and (e) Fe_3O_4+Triton X100.

Table 1. Comparing Crystal size (nm), Pos. [°2Th.], FWHM [°2Th.] and Rel. Int. [%] before and after adding the surfactant.

Samples	Crystal size\(nm)	Pos. [°2Th.]	FWHM [°2Th.]	Rel. Int. [%]
Fe_3O_4	8.5 nm	36.6237	0.6794	100
		62.9711	0.4491	63.96
		58.9639	0.3163	53.56
Fe_3O_4 +Triton X 100	21.55	35.66	0.384	100
		62.764	0.384	63.21
		57.2672	0.576	32.12
Fe_3O_4 +CTAB	27.72	35.5271	0.192	100
		62.7934	0.48	58.5
		57.1004	0.577	39.45
Fe_3O_4 + SDS	27.66	35.5259	0.288	100
		62.77	0.336	52.44
		57.1619	0.384	32.41
Fe_3O_4+ CT	22.53	35.5847	0.288	100
		62.9704	0.48	72.61
		36.7305	0.576	52.03

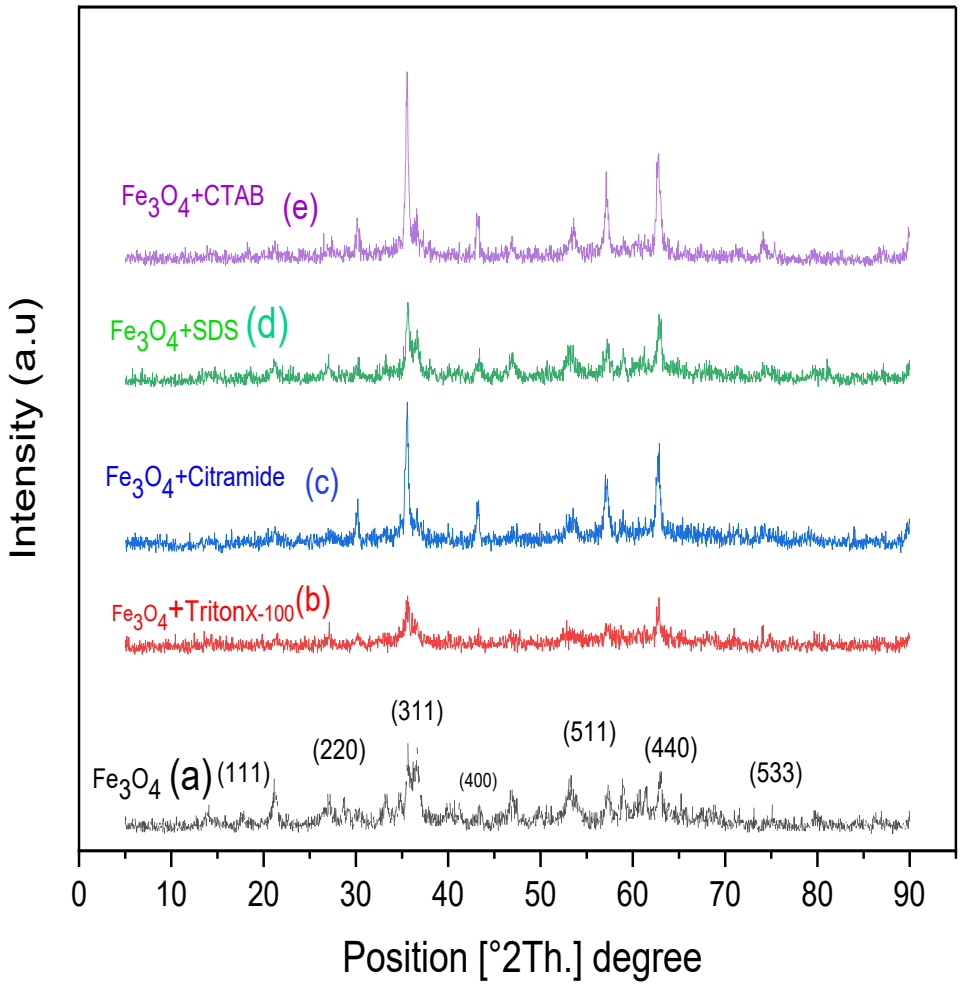

Fig. 4. The XRD spectrum of magnetite without and with its surfactants(a) Fe_3O_4 , (b) Fe_3O_4+Triton X-100, (c) Fe_3O_4+CT, (d) Fe_3O_4 +,SDS and (e)Fe_3O_4 +CTAB.

(JCPDS No. 19-0629) [18].

Based on data in Table 1, the mean crystal sizes of the synthesized magnetite nanoparticles without and with addition of surfactants were calculated using Debye-Scherer formula [19-26].

$$D = \frac{K\lambda}{\beta \cos \theta} \quad (3)$$

Where D = the mean diameter of nanoparticles, β is the full width at half-maximum value of XRD diffraction lines, = the wavelength of X-ray radiation source 0.15405 nm. = the half diffraction angle –Bragg angle and k = the Scherer constant with value from 0.84 to 0.94.

The mean crystal size of Fe_3O_4 NP was 8.5 nm that regarded as a quantum dote nanoparticle because its size value is less than 10 nm. This same crystal size has been observed in other studies that have reported in references [27-29]. However, after adding the surfactants during Fe_3O_4 NP preparation, the mean crystal size increases due to behaviour of surfactants as a template. The surfactants are surrounds of Fe_3O_4 NP, so, the hydrophobic terminals are being around the crystal of Fe_3O_4 NP, but the hydrophilic terminals are being far toward a solution, that attitude to dissolve the surfactants in the aqueous solutions then it leads to increase the value of mean crystal size of Fe_3O_4 NP. Furthermore, addition of the surfactant protects the Fe_3O_4 NP from the agglomeration before adding the surfactants because their small size and magnetic properties.

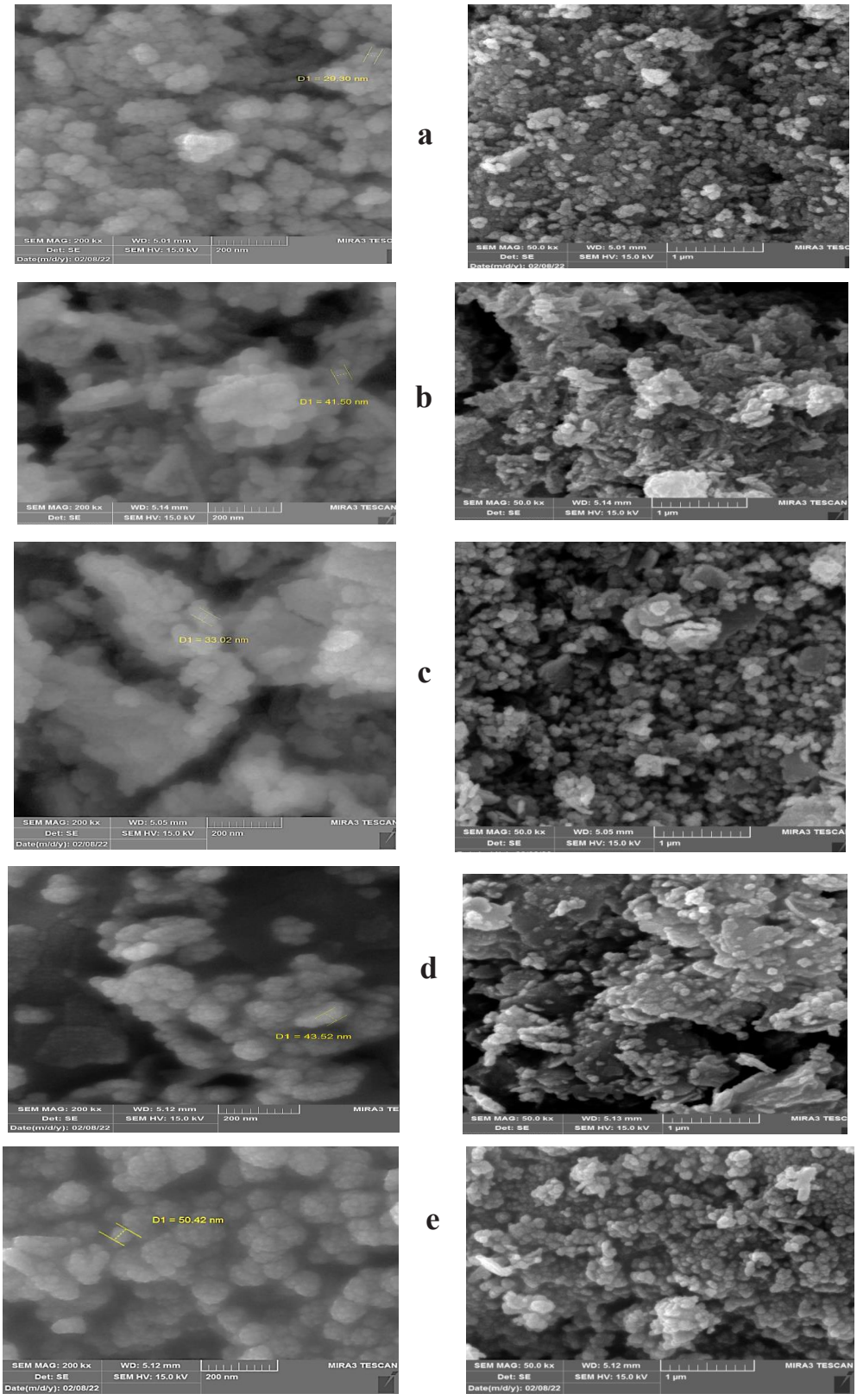

Fig. 5. The scanning electron microscope (SEM) for (a) Fe_3O_4 and (b) Fe_3O_4+SDS (c)Fe_3O_4+Triton X-100 and (d) Fe_3O_4 +CTAB (e) Fe_3O_4 +CT.

SEM analysis

Scanning Electron Microscope (SEM) is one of the most important techniques for studying various surfaces and the changes that occur on them. In this study, the SEM micrograph of the adsorbent shows morphological characteristics that are favourable for metal adsorption.

From Fig. 5 (a-e), the small Fe_3O_4 NP are agglomerated and are like-broccoli with large size, and the particle size of Fe_3O_4 NP without and with addition of surfactants found the values increase with the following sequences: (20-30 nm), (41-50 nm), (43-5 nm),(42-50 nm),and (42-50 nm) for Fe_3O_4 NP, and with SDS, triton X100, CTAB and CT, respectively. This behaviour refers to all prepared NP as poly-crystals, these results are in agreement with the other results that have been reported in [30-33].

Application of magnetic nanoparticles for removal of Eosin yellow dye

The synthesized nanoparticles were used in the removal of eosin yellow dye as a water contamination. Fig. 6 illustrates the E removal % for using Fe_3O_4 raises after using surfactants at the different of dye concentrations 10 and 25 ppm. The removal of the high concentration of dye (25 ppm) was faster than the removal of low concentration of dye 10 ppm, that attitude is due to the increment in the number of collisions of the dye ions with the catalyst surface (Fe_3O_4 NPs) during adsorption process [34]. The best E removal % is found after using Fe_3O_4 + CT as a surfactant equal to 94.7 % at 25 ppm dye and 0.05 g of NP, and equal to 94.6 % at 10 ppm dye with 0.05 g NP. Also, In Fig. 7, the adsorption capacity (q) for using Fe_3O_4 raises after using CT as a surfactant and the q maximum was 2.37 mg/g when using 25 ppm with 0.05 g of then nanoparticle, and 0.95 mg/g when using 10 ppm with 0.05 g. The using of CT as a positive surfactant gives the best removal results which is due to the acidity the dye so the attractive forces will increase on Fe_3O_4 NP, that was prepared in presence of a CT, the role of using CT via Fe_3O_4 NP preparation can be displayed in Fig. 8, that based on the hydrophobic part of this surfactant is binding with the surface of Fe_3O_4 because it surface is neutral, while the dye attractive with the hydrophilic part of surfactant that have a positive charge in aqueous solution [11]. The negative parts in dye will attract with the positive charge of surfactant and enhanced the removal of dye from aqueous solution.

The nanoparticles that synthesized magnetite

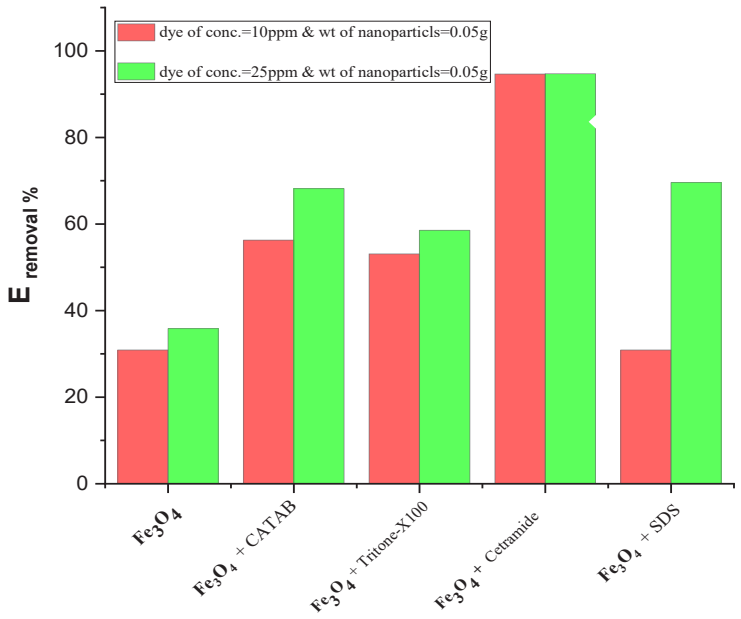

Fig. 6. Relationship between the E % of the dye removed and synthesized Fe_3O_4 NP with different surfactants at 60 minute

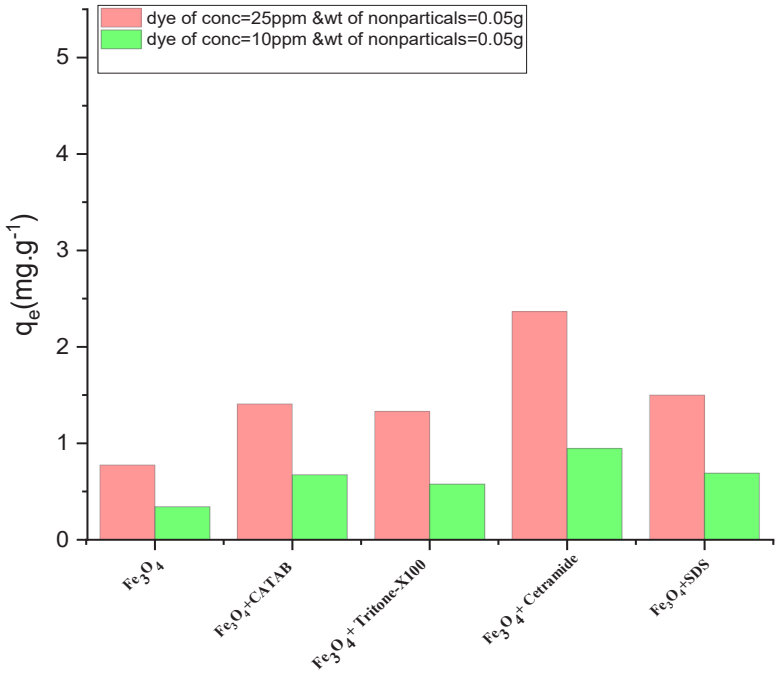

Fig. 7. The relationship between adsorption capacity and the type of nanoparticles produced by various surfactants.

with CT had the highest q.

The effectiveness of nanoparticles synthesized with the cetramide surfactant

Because of adsorption of eosin yellow dye by Fe_3O_4 NP which are synthesized by presence of the surfactant. That can be behaved as reverse process and it is adsorption process will decrease with reuse for several times. This observation can be obtained during the saturated process of the active site of the synthesized nanoparticles which will be occupied by the particles of the dye. The removed eosin yellow dye from aqueous solutions decreases from 94.48% in the first stage to 75.61 % (Fig. 9), when the repeating five times this regards a good percentage, also the amount of adsorption of the dye decreases from 4.72 mg/g to 3.75 mg/g and this indicates that 0.01 g from the nanoparticles has the ability to be reused several times, but the activity of nanoparticles decreases in small amounts when the repeating for many times as shown in the Fig. 10.

Effect of temperature on removal of dye

Temperature is one of the factors affecting the removal of the dye by magnetite nanoparticles and it also affects the structure of the dye sometimes. The effect of temperature from (5 to 50) °C were studied on both the adsorption capacity of dye and the E removal % from (10-60) minutes of incubation time. The results in figure 13 were observed that the removal values increase with increasing the temperature from 5 °C to 30 °C. This behave demonstrates that the increased in the temperature will raise the mobility and the kinetic energy of dyes'molecul in the solution, to reach easy for the active sites surface that increase the dye affinity for adsorbed on catalyst surface [34,35]. On the other hand, the E removal % decreases at high temperatures such as 40°C and 50°C. The reason is related to the increase of the concentration of the dye with increasing in the temperature (40-50) °C which is lead to increase in the vaporization of the aqueous solutions. As shown in Fig. 11.

The thermodynamics parameters are vital parameters in the investigation the type of the adsorption process that happened on any solid surface. In outset, sorption distribution coefficient (kd) [13,35] was found using equation 4, when $C_{ads.}$ is the amount of adsorbate (dye) on the solid surface of the Fe_3O_4 NPs CT at

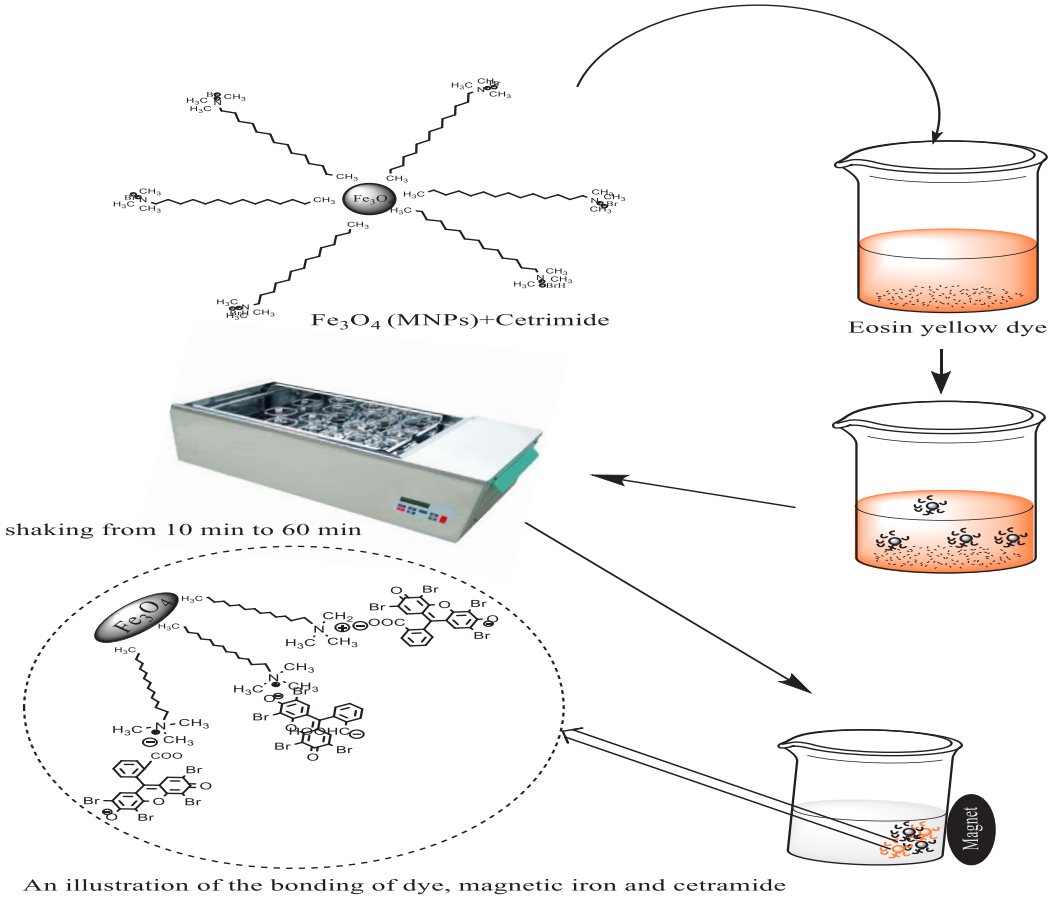

Fig. 8. Mechanism of removal the dye from its solutions using Fe_3O_4 NP in presence of surfactant.

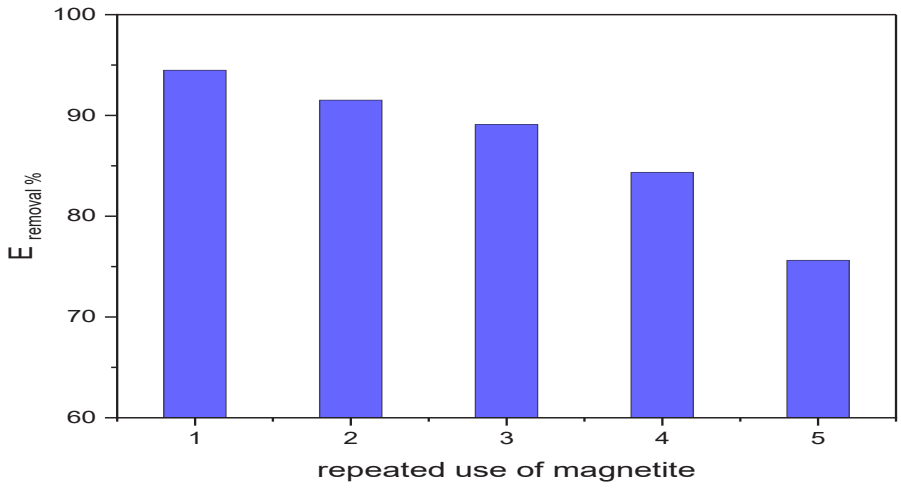

Fig. 9. The effectiveness of Fe_3O_4 nanoparticles that prepared in presence of CT on the removal of dye for five times.

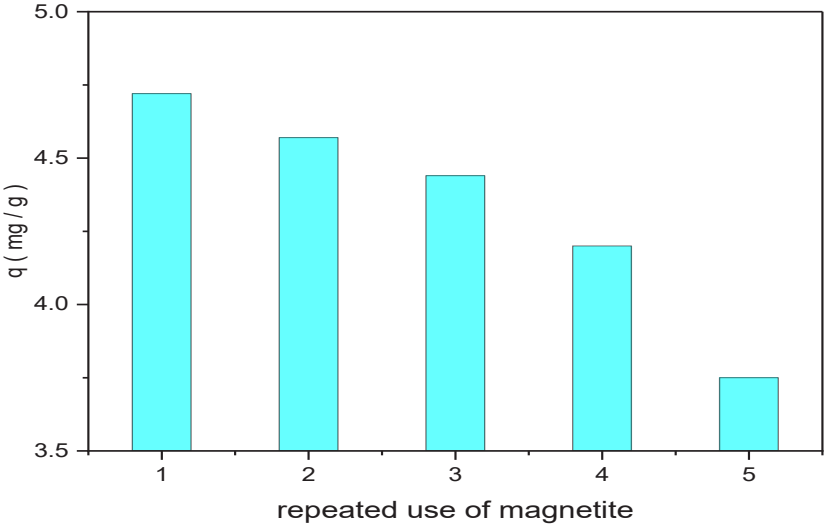

Fig. 10. The relationship between the amount of dye that adsorbs on the Fe_3O_4NPs sizes in presence of a CT in mg/g via the repeat of using Fe_3O_4 NP sizes in presence of a CT in several times.

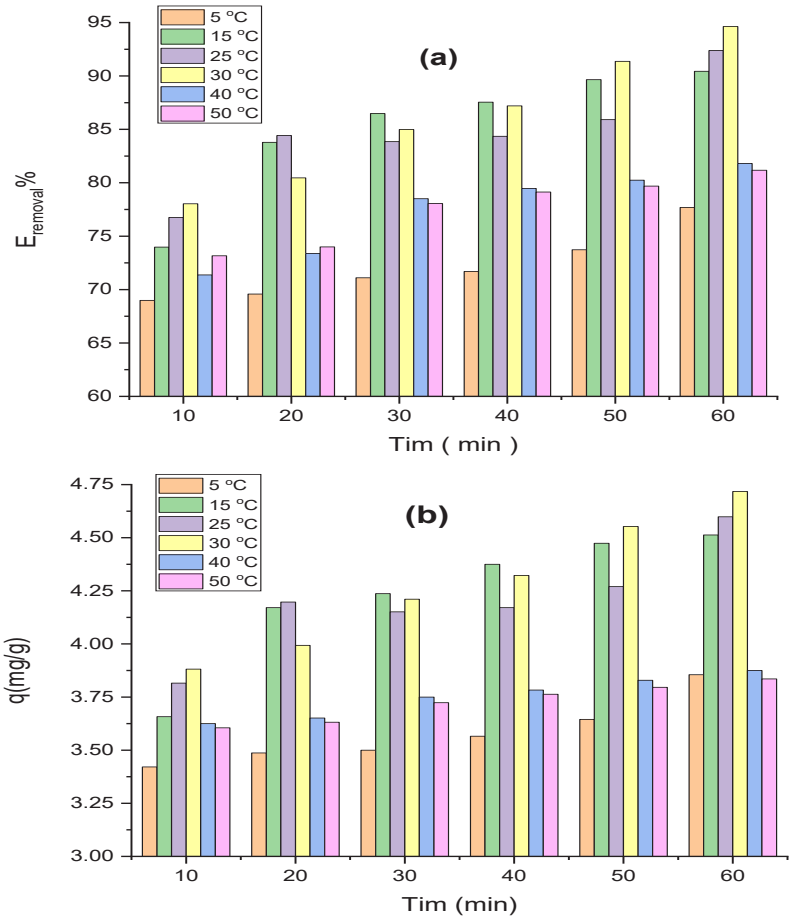

Fig. 11. The effect of the temperature on the removal of the dye using iron oxide NP that synthesized in presence of the CT surfactant. a) Plotted E % with the time b) plotted q with the time.

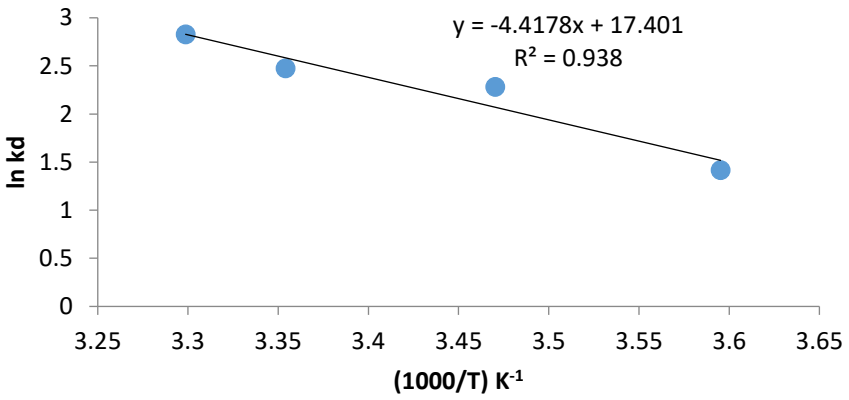

Fig. 12. Relation between ln k_d and (1000/T) for adsorption of eosin yellow dye on Fe_3O_4 surface that prepared in presence of CT as a surfactant at 1h.

Table 2. The Kinetic and Thermodynamic Parameters for Adsorption of Eosin Yellow Dye on Fe_2O_4 NPs+ CT.

(1000/T)	Ln k_d	ΔH° kJ mol^{-1}	ΔS° kJ mol^{-1}	ΔG° kJ mol^{-1}	T/K	E_a kJ mol^{-1}
3.597	-1.053	36.729	0.144	-3.273	278	39.040
3.472	-2.091			-5.463	288	39.124
3.355	-2.305			-6.134	298	39.207
3.300	-2.684			-7.122	303	39.248

equilibrium (mg/L). Ce is a residual dye (mg/L) in a solution at equilibrium. The standard Gibbs free energy (ΔG°) was calculated [15,36] using equation 5 (Gibbs equation), when R is universal gas constant (J/mol K) and T is the absolute temperature in Kelvin.

$$k_d = \frac{C_{ads.}}{C_e} \quad (4)$$

$$\Delta G^o = -RT\ln k_d \quad (5)$$

The change in the standard enthalpy ΔH° and change in standard entropy ΔS ° were measured [37,38] using the Van't Hoff equation (equation 6).

$$\ln k_d = \frac{-\Delta H^o}{RT} + \left(\frac{\Delta S^o}{R}\right) \quad (6)$$

On the other hand, the activation energy was calculated using equation 7 [15, 38].

$$E_a = \Delta H^o + RT \quad (7)$$

Based on the results in Fig. 12 and Table 2, the positive magnitude of ΔH° value for the adsorption process of eosin yellow dye on Fe_3O_4 NP /CT surface is found to be endothermic nature and equal to (36.729 kJ mol^{-1}). This value reveals the adsorption process is chemisorption because it has the value which is a more than 20 kJ mol^{-1}[37]. Moreover, the ΔS° magnitudes is small and positive (0.14467 kJ mol^{-1}) that implied the randomness on the solid/solution interface raises, hence the mechanism of adsorption take place as an associative mechanism with change in the internal structure [37]. In Table 2, the positive values of activation energies increase with increasing the temperature within the range of (39.040 - 39.248) kJ mol^{-1} that proved the process is chemisorption. This observation is based on the calculated that E_a was between 8.4 kJ mol^{-1} and 83.7 kJ mol^{-1}[37], which is given chemisorption.

In Fig. 13, the increased in temperature caused depress in a negative ΔG° magnitudes within the range of (-7.122 mol^{-1} to -3.273) kJ mol^{-1} that indicates to this reaction is favour, spontaneous and not required to energy from an external

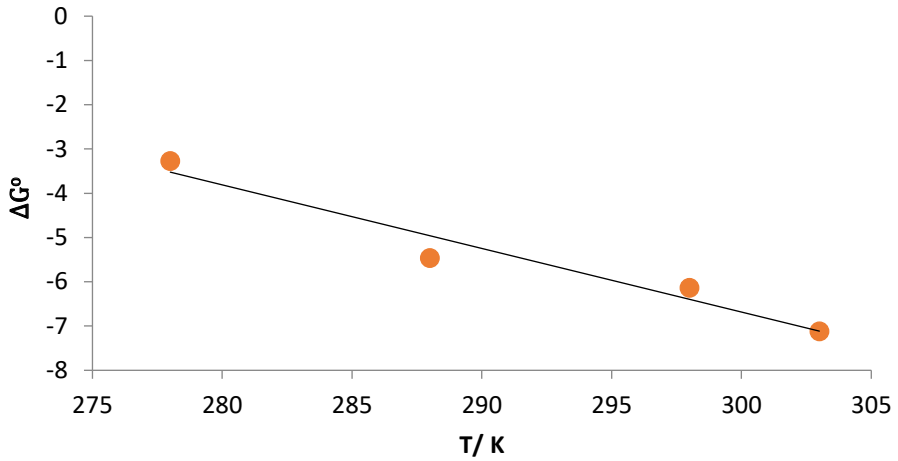

Fig. 13. Relation of standard Gibb's free energy change (DG°) versus temperature for an exothermic process of adsorption of eosin yellow dye on Fe_3O_4 surface that prepared in presence of CT as a surfactant in temperature ranged (278.15-303.15) K at 1h.

source to convert reactants into products [37]. The thermodynamics results are in agreement with the similar results that had been reported previously [33].

CONCLUSION

During this study, magnetic iron oxide nanoparticles were prepared in the presence and absence of surfactants in their aqueous solutions. It was observed that the size of the magnetic iron oxide nano- crystals increases in presence of surfactants. XRD data indicated that the preparation of Fe_3O_4 NPs in small nano-size as quantum dots nanoparticle, and raised the nano-size after using various surfactants. The SEM analysis was found that all samples are nanoparticle and can be agglomerated to give like-broccoli shapes. FT-IR analysis occurred that t h e magnetic iron oxide nanoparticle is spinel based on positions of octahedron (Fe-O) site and tetrahedral (Fe-O) site peaks. The possibility of using the prepared magnetic nanoparticles as magnetic adsorbents in removing the eosin yellow dye from aqueous solutions was estimated. The best E removal % was found after using iron oxide NP equal to 94.48 % that prepared in the presence of CT at 25 ppm dye, 0.01 g catalyst, pH 7, 30 °C and 1 hour of the shaking process. The study also dealt with the possibility of using the prepared iron oxide more than once to remove eosin yellow dye, and it was found that nanoparticles maintain their adsorption efficiency when used several times with a small decrease in the extraction efficiency. It also dealt with the effect of temperature in the adsorption process and its impact on the efficiency of the removed dye, when it was noted that 30 °C is the best degree for dye removal. The adsorption process for eosin yellow dye on Fe_3O_4 prepared in presence of CT found as chemisorption in nature, with positive enthalpy and entropy.

ACKNOWLEDGMENTS

The Authors would like to thank all personnel who support this manuscript in the University of Kerbala's faculty.

CONFLICT OF INTEREST

The authors declare that there is no conflict of interests regarding the publication of this manuscript.

REFERENCES

1. Serbin LA, Peters PL, Schwartzman AE. Longitudinal study of early childhood injuries and acute illnesses in the offspring of adolescent mothers who were aggressive, withdrawn, or aggressive–withdrawn in childhood. J Abnorm Psychol. 1996;105(4):500-507.
2. Cordova G, Attwood S, Gaikwad R, Gu F, Leonenko Z. Magnetic Force Microscopy Characterization of Superparamagnetic Iron Oxide Nanoparticles (SPIONs). Nano Biomed Eng. 2014;6(1).

3. Cornell RM, Schwertmann U. The Iron Oxides: Wiley; 2003 2003/07/29.
4. Mohapatra M, Anand S. Synthesis and applications of nano-structured iron oxides/hydroxides – a review. International Journal of Engineering, Science and Technology. 2011;2(8).
5. Astanina K, Simon Y, Cavelius C, Petry S, Kraegeloh A, Kiemer AK. Superparamagnetic iron oxide nanoparticles impair endothelial integrity and inhibit nitric oxide production. Acta Biomater. 2014;10(11):4896-4911.
6. Alizadeh T, Jahani R. A new strategy for low temperature gas sensing by nano-sized metal oxides: Development a new nerve agent simulant sensor. Materials Chemistry and Physics. 2015;168:180-186.
7. Liu G, Cai M, Wang X, Zhou F, Liu W. Magnetite-Loaded Thermosensitive Nanogels for Bioinspired Lubrication and Multimodal Friction Control. ACS Macro Lett. 2016;5(1):144-148.
8. De Martino MT, Abdelmohsen LKEA, Rutjes FPJT, van Hest JCM. Nanoreactors for green catalysis. Beilstein J Org Chem. 2018;14:716-733.
9. Zapol WM. Extracorporeal Membrane Oxygenation in Severe Acute Respiratory Failure. JAMA. 1979;242(20):2193.
10. Iwasaki T. Mechanochemical Synthesis of Water-Based Magnetite Magnetic Fluids. Magnetic Spinels - Synthesis, Properties and Applications: InTech; 2017.
11. Ahmed LM. Photo-Decolourization Kinetics of Acid Red 87 Dye in ZnO Suspension Under Different Types of UV-A Light. Asian J Chem. 2018;30(9):2134-2140.
12. Hussain ZA, Fakhri FH, Alesary HF, Ahmed LM. ZnO Based Material as Photocatalyst for Treating the Textile Anthraquinone Derivative Dye (Dispersive Blue 26 Dye): Removal and Photocatalytic Treatment. Journal of Physics: Conference Series. 2020;1664(1):012064.
13. Jawad TM, R. Al-Lami M, Hasan A, Al-Hilifi J, Mohammad R, Ahmed L. Synergistic Effect of dark and photoreactions on the removal and photo-decolorization of azo carmosine dye (E122) as food dye using Rutile- TiO_2 suspension. Egyptian Journal of Chemistry. 2021;0(0):0-0.
14. Alattar R, Saleh H, Al-Hilifi J, Ahmed L. Influence the addition of Fe^{2+} and H_2O_2 on removal and decolorization of textile dye (dispersive yellow 42 dye). Egyptian Journal of Chemistry. 2020;0(0):0-0.
15. Ding Y, Yang Y, Shao H. High capacity $ZnFe_2O_4$ anode material for lithium ion batteries. Electrochimica Acta. 2011;56(25):9433-9438.
16. Luo X, Liu S, Zhou J, Zhang L. In situ synthesis of Fe_3O_4/cellulose microspheres with magnetic-induced protein delivery. Journal of Materials Chemistry. 2009;19(21):3538.
17. Ramesh AV, Rama Devi D, Mohan Botsa S, Basavaiah K. Facile green synthesis of Fe_3O_4 nanoparticles using aqueous leaf extract of *Zanthoxylum armatum* DC. for efficient adsorption of methylene blue. Journal of Asian Ceramic Societies. 2018;6(2):145-155.
18. Jawad TM, Ahmed LM. DIRECT ULTRASONIC SYNTHESIS OF WO_3/TiO_2 NANOCOMPOSITES AND APPLYING THEM IN THE PHOTODECOLORIZATION OF EOSIN YELLOW DYE. Periódico Tchê Química. 2020;17(34):621-633.
19. Ahmed L, Ali S, Ali M. Hybrid Phosphotungstic acid -Dopamine (PTA-DA) Like-flower Nanostructure Synthesis as a Furosemide Drug Delivery System and Kinetic Study of Drug Releasing. Egyptian Journal of Chemistry. 2021;0(0):0-0.
20. Ridha NJ, Mohamad Alosfur FK, Kadhim HBA, Ahmed LM. Synthesis of Ag decorated TiO_2 nanoneedles for photocatalytic degradation of methylene blue dye. Materials Research Express. 2021;8(12):125013.
21. Ahmed L, Alkhafaji E, Oda N. Characterization of silver nanohybrid with layers double hydroxide and demonstration inhibition of antibiotic-resistance Staphylococcus aureus. Egyptian Journal of Chemistry. 2022;0(0):0-0.
22. Solution Combustion Synthesis, Characterization, and Photocatalytic Activity of $CuBi_2O_4$ and Its Nanocomposites with CuO and Bi2O3. American Chemical Society (ACS).
23. Jassim S, Abbas A, Al-Shakban M, Ahmed L. Chemical Vapour Deposition of CdS Thin Films at Low Temperatures from Cadmium Ethyl Xanthate. Egyptian Journal of Chemistry. 2021;64(5):3-4.
24. Abed z, Mohammad R, Elttayef A. Structural properties of Ag-CuO thin films on silicon prepared via DC magnetron sputtering. Egyptian Journal of Chemistry. 2021;0(0):0-0.
25. Fakhri FH, Ahmed LM. Incorporation CdS with ZnS as Composite and Using in Photo-Decolorization of Congo Red Dye. Indonesian Journal of Chemistry. 2019;19(4):936.
26. Han C, Li Z, Shen J. Photocatalytic Producation of Hydrogen from Aqueous Methanol Solution over Pt/TiO_2-Cu_2O Under Visible Irradiation. Asian J Chem. 2015;27(5):1861-1864.
27. Ahmed LM, Ivanova I, Hussein FH, Bahnemann DW. Role of Platinum Deposited on TiO_2 in Photocatalytic Methanol Oxidation and Dehydrogenation Reactions. International Journal of Photoenergy. 2014;2014:1-9.
28. Ahmed L, Kadhim H, Al-Hachamii M. Facile Synthesis of Spinel $CoCr_2O_4$ and Its Nanocomposite with ZrO_2: Employing in Photo-catalytic Decolorization of Fe (II)-(luminol-Tyrosine) Complex. Egyptian Journal of Chemistry. 2021;0(0):0-0.
29. Obaid A, Ahmed L. One-Step Hydrothermal Synthesis of α-MoO_3 Nano-belts with Ultrasonic Assist for incorporating TiO_2 as a NanoComposite. Egyptian Journal of Chemistry. 2021;0(0):0-0.
30. Hayawi MK, Kareem MM, Ahmed LM. SYNTHESIS OF SPINEL Mn3O4 AND SPINEL Mn_3O_4/ZrO_2 NANOCOMPOSITES AND USING THEM IN PHOTO-CATALYTIC DECOLORIZATION OF Fe(II)-(4,5- DIAZAFLUOREN-9-ONE 11) COMPLEX. Periódico Tchê Química. 2020;17(34):689-699.
31. Surinwong S, Rujiwatra A. Ultrasonic cavitation assisted solvothermal synthesis of superparamagnetic zinc ferrite nanoparticles. Particuology. 2013;11(5):588-593.
32. Al-Senani GM, Al-Fawzan FF, Almufarij RS, Abd-Elkader OH, Deraz NM. Biosynthesis, Physicochemical and Magnetic Properties of Inverse Spinel Nickel Ferrite System. Crystals. 2022;12(11):1542.
33. Karam F, Saeed N, Al Yasasri A, Ahmed L, Saleh H. Kinetic Study for Reduced the Toxicity of Textile Dyes (Reactive yellow 14 dye and Reactive green dye) Using UV-A light/ZnO System. Egyptian Journal of Chemistry. 2020;0(0):0-0.
34. Sadeghi M, Irandoust M, Khorshidi F, Feyzi M, Jafari F, Shojaeimehr T, et al. Removal of Arsenic (III) from natural contaminated water using magnetic nanocomposite: kinetics and isotherm studies. Journal of the Iranian Chemical Society. 2016;13(7):1175-1188.
35. Jaafar MT, Ahmed LM. Reduced the toxicity of acid black (nigrosine) dye by removal and photocatalytic activity of TiO_2 and studying the effect of pH, temperatue, and the oxidant agents. INTERNATIONAL CONFERENCE OF NUMERICAL ANALYSIS AND APPLIED MATHEMATICS ICNAAM 2019: AIP Publishing; 2020.

36. Saha P, Chowdhury S. Insight Into Adsorption Thermodynamics. Thermodynamics: InTech; 2011.
37. Zarrouk A, Hammouti B, Zarrok H, Al-Deyab SS, Warad I. Thermodynamic study of metal corrosion and inhibitor adsorption processes in copper/N-1-naphthylethylenediamine dihydrochloride monomethanolate/nitric acid system: part 2. Res Chem Intermed. 2012;38(7):1655-1668.